modulator. Thioredoxin also has an extracellular function as a secreted form, displaying many of the activities of interleukin-1 (IL-1) (*22*). Alternatively, since IL-1 can induce the production of free radicals (*27*), it is possible that thioredoxin (acting like IL-1) and IFN-γ together could induce inhibitory concentrations of free radicals. The challenge now is to determine whether these effects, or others, are significant during the growth arrest of HeLa cells.

REFERENCES AND NOTES

1. G. Klein, *Science* **238**, 1539 (1987); R. A. Weinberg, *Cancer Res.* **49**, 3713 (1989); R. Sager, *Science* **246**, 1406 (1989); T. Mikkelsen and W. K. Cavenee, *Cell Growth Differ.* **1**, 201 (1990).
2. S. Friend *et al.*, *Nature* **323**, 643 (1986); P. S. Steg, G. Bevilaqua, A. M. Rosengard, V. Croce, L. A. Liotta, *Cancer Res.* **48**, 6550 (1988); R. Schaefer, J. Iyer, E. Iten, A. C. Nirkko, *Proc. Natl. Acad. Sci. U.S.A.* **85**, 1590 (1988); C. A. Findlay, P. W. Hinds, A. Levine, *Cell* **57**, 1083 (1989); D. Eliyahu, D. Michaelovitch, S. Eliyahu, O. Pinhasi-Kimchi, M. Oren, *Proc. Natl. Acad. Sci. U.S.A.* **86**, 8763 (1989); M. Noda *et al.*, *ibid.*, p. 162; E. R. Fearon *et al.*, *Science* **247**, 49 (1990).
3. P. Lengyel, *Annu. Rev. Biochem.* **51**, 521 (1982); P. Gray *et al.*, *Nature* **312**, 721 (1984); D. Pennica *et al.*, *ibid.*, p. 724; R. Derynck *et al.*, *ibid.* **316**, 701 (1985); N Malik *et al.*, *Mol. Cell. Biol.* **9**, 2847 (1987); M. Shoyab, G. D. Plowman, V. L. McDonald, J. G. Bradley, G. J. Todaro, *Science* **243**, 1074 (1989).
4. D. Resnitzky, A. Yarden, D. Zipori, A. Kimchi, *Cell* **46**, 31 (1986); J. A. Bernard, R. D. Beauchamp, R. J. Coffey, H. L. Moses, *Proc. Natl. Acad. Sci. U.S.A.* **86**, 1578 (1989).
5. M. O. Diaz *et al.*, *Proc. Natl. Acad. Sci. U.S.A.* **85**, 5259 (1988).
6. M. Einat, D. Resnitzky, A. Kimchi, *Nature* **313**, 597 (1985).
7. M. Einat and A. Kimchi, *Oncogene* **2**, 485 (1988); J. A. Pietenpol, J. T. Holt, R. W. Stein, H. L. Moses, *Proc. Natl. Acad. Sci. U.S.A.* **87**, 3758 (1990); J. A. Pietenpol *et al.*, *Cell* **61**, 777 (1990); D. Resnitzky and A. Kimchi, *Cell Growth Differ.* **2**, 33 (1991).
8. A. Yarden and A. Kimchi, *Science* **234**, 1419 (1986).
9. A. Kimchi, D. Resnitzky, R. Ber, G. Gat, *Mol. Cell. Biol.* **8**, 2828 (1988).
10. J. N. M. Ijzermans and R. C. Marquet, *Immunobiology* **179**, 456 (1989).
11. Y. Watanabe *et al.*, *Proc. Natl. Acad. Sci. U.S.A.* **86**, 9456 (1989).
12. J. L. Yates, N. Warren, B. Sugden, *Nature* **313**, 812 (1985); N. R. Drinkwater and D. K. Klinedinst, *Proc. Natl. Acad. Sci. U.S.A.* **83**, 3402 (1986); R. K. Groger, D. M. Morrow, M. L. Tykocinski, *Gene (Amst.)* **81**, 285 (1989). Groger *et al.* have independently reported the construction of an anti-sense cDNA library cloned into an EBV vector.
13. F. Graham and A. Van der Eb, *Virology* **52**, 456 (1973).
14. B. Hirt, *J. Mol. Biol.* **26**, 365 (1967).
15. B. Cohen, D. Peretz, D. Vaiman, P. Benech, J. Chebath, *EMBO J.* **7**, 1411 (1988).
16. L. P. Deiss and A. Kimchi, unpublished results.
17. U. Gubler and B. J. Hoffman, *Gene (Amst.)* **25**, 263 (1983).
18. P. S. Meissner, W. P. Sisk, M. L. Berman, *Proc. Natl. Acad. Sci. U.S.A.* **84**, 4171 (1987).
19. The cDNA library was constructed from 10 μg of oligo(dT)-selected mRNA by the method of Gubler and Hoffman (*17*). The resulting dscDNA was methylated by Bam HI and Alu I methylases and ligated to the linker described by Meisner *et al.* (*18*). Briefly, the ligation to the polyadenylated end of the cDNA generates a Hind III site, whereas at the 5′ end of the cDNA a Bam HI site is generated. This was followed by cleavage with Bam HI and Hind III and purification on an S-400 spin column (Promega). The purified dscDNA was ligated, at a 3:1 ratio, to Hind III– and Bgl II–cleaved pTKO1, and the ligation mixture was used to transform a variant of HB101 (obtained from M. Oren). The pTKO1 was generated by digestion of pTKO1-DHFR with Hind III and Bgl II, and dephosphorylation followed by preparative gel electrophoresis. The HB101 was made competent by the method of D. Hanahan [*J. Mol. Biol.* **166**, 557 (1983)], except that the dimethyl sulfoxide step was omitted.
20. D. J. Bergsma, D. M. Olive, S. W. Hartzwell, K. N. Subramanian, *Proc. Natl. Acad. Sci. U.S.A.* **79**, 381 (1982).
21. Y. Tagaya *et al.*, *EMBO J.* **8**, 757 (1989). The cDNA segment, containing 291 bp of open reading and 51 bp of the 5′ untranslated region, matched this sequence exactly and extended from nucleotide 29 to 371 (numbering system of Tagaya *et al.*).
22. E. E. Wollman *et al.*, *J. Biol. Chem.* **263**, 15506 (1988). The cDNA segment was extended from nucleotide 12 to 354 (numbering system of Wollman *et al.*). Two discrepancies occur at nucleotide 180 and 284 (numbering of Wollman *et al.*) and result in two amino acid changes. The functional significance of these changes is unknown.
23. P. Boukamp *et al.*, *J. Cell Biol.* **106**, 761 (1988).
24. A. Holmgren, *Annu. Rev. Biochem.* **54**, 237 (1985); *J. Biol. Chem.* **264**, 13963 (1989).
25. T. M. Aune and S. Pogue, *J. Clin. Invest.* **84**, 863 (1989).
26. C. F. Bennett, J. M. Balcarek, A. Varrichio, S. T. Crooke, *Nature* **334**, 268 (1988); J. F. Grippo, A. Holmgren, W. B. Pratt, *J. Biol. Chem.* **260**, 93 (1985); C. Abate, D. Luk, R. Gentz, F. J. Rauscher, T. Curran, *Proc. Natl. Acad. Sci. U.S.A.* **87**, 1032 (1990); C. Abate, L. Patel, F. J. Rauscher III, T. Curran, *Science* **249**, 1157 (1990).
27. J. M. Brown *et al.*, *Proc. Natl. Acad. Sci. U.S.A.* **87**, 5026 (1990).
28. F. Lee, R. Mulligan, P. Berg, G. Ringold, *Nature* **294**, 228 (1981).
29. R. W. Ellis *et al.*, *J. Virol.* **36**, 408 (1980).

30. We thank B. Sugden for the gift of p220.1 and J. Chebath for the gift of the multimer of the human IRS. We thank D. Reisman for technical advice, helpful discussions, and for encouraging us to use the EBV vector. We thank M. Rubinstein and D. Novick for the human IFN-γ. This work was supported by Leo and Julia Forchheimer Center for Molecular Genetics and by Minerva.

5 October 1990; accepted 9 January 1991

Selective Activation of the B Natriuretic Peptide Receptor by C-Type Natriuretic Peptide (CNP)

KERRY J. KOLLER,* DAVID G. LOWE, GREGORY L. BENNETT, NAOTO MINAMINO, KENJI KANGAWA, HISAYUKI MATSUO, DAVID V. GOEDDEL

The natriuretic peptides are hormones that can stimulate natriuretic, diuretic, and vasorelaxant activity in vivo, presumably through the activation of two known cell surface receptor guanylyl cyclases (ANPR-A and ANPR-B). Although atrial natriuretic peptide (ANP) and, to a lesser extent, brain natriuretic peptide (BNP) are efficient activators of the ANPR-A guanylyl cyclase, neither hormone can significantly stimulate ANPR-B. A member of this hormone family, C-type natriuretic peptide (CNP), potently and selectively activated the human ANPR-B guanylyl cyclase. CNP does not increase guanosine 3′,5′-monophosphate accumulation in cells expressing human ANPR-A. The affinity of CNP for ANPR-B is 50- or 500-fold higher than ANP or BNP, respectively. This ligand-receptor pair may be involved in the regulation of fluid homeostasis by the central nervous system.

ANP WAS THE FIRST DESCRIBED member of a family of polypeptide hormones that regulates salt and water balance and blood pressure (*1*). Subsequent to the isolation and characterization of ANP, two related hormones have been described: BNP, isolated from both brain and heart (*2, 3*), and CNP, purified from porcine brain (*4*). Like ANP, both of these hormones can elicit vasorelaxant, natriuretic, and diuretic responses in chick and rat bioassay systems (*2, 4*). These natriuretic peptides share a common structural motif consisting of a 17–amino acid loop formed by an intramolecular disulfide linkage. Only 5 of the 17 amino acids in the ring differ among the three peptides isolated from the pig, whereas the NH_2- and COOH-terminals vary in both amino acid composition and length (*4*). Among different species, the structures of both ANP and CNP are highly conserved (*1, 5*), whereas the amino acid sequence of BNP varies as much as 50% (*2, 3, 6*).

The biological activities of the natriuretic peptides are thought to be mediated by intracellular accumulation of guanosine 3′,5′-monophosphate (cGMP) through the activation of particulate guanylyl cyclase (*1, 7, 8*). Molecular cloning studies have identified three distinct natriuretic peptide receptors. ANPR-A and ANPR-B (also called

K. J. Koller, D. G. Lowe, D. V. Goeddel, Department of Molecular Biology, Genentech, Inc., South San Francisco, CA 94080.
G. L. Bennett, Department of Immunology Research and Assay Technology, Genentech, Inc., South San Francisco, CA 94080.
N. Minamino and H. Matsuo, National Cardiovascular Center Research Institute, Fujishirodai, Suita, Osaka 565, Japan.
K. Kangawa, Department of Biochemistry, Miyazaki Medical College, Kihara, Kiyotake, Miyazaki 889-16, Japan.

*To whom correspondence should be addressed.

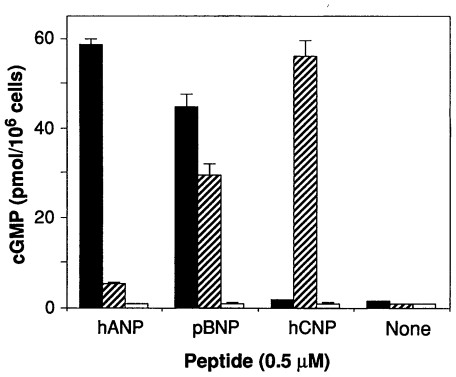

Fig. 1. Whole-cell stimulation of COS-7 cells transiently expressing the receptor guanylyl cyclases. COS-7 cells were plated in six-well dishes (2.5 × 10^5 cells per well) 18 hours before transfection by lipofection with the appropriate receptor plasmid DNA (ANPR-A, solid bars; ANPR-B, hatched bars; or expression vector, open bars; 1.5 μg of DNA and 15 μg of lipofectin reagent per well) as per manufacturer's instructions (Gibco–Bethesda Research Labs.). Forty-eight hours after addition of DNA, cells were washed once with DMEM + Hepes (25 mM, pH 7.2), incubated with DMEM + Hepes (25 mM, pH 7.2) + isobutyl methylxanthine (0.1 mM) (D/H/I) for 10 min at 37°C, and incubated for 5 min at 37°C in D/H/I with or without 0.5 μM of the appropriate peptide. Stimulation for longer than 5 min did not increase the concentration of cGMP produced (data not shown). The incubation media was aspirated and replaced with 1 ml of 10% trichloroacetic acid, and the cells were frozen quickly on dry ice. After the samples thawed at room temperature, the cell debris was removed by centrifugation at 2500*g* for 10 min. Samples were extracted three times with 500 μl of water-saturated ether and warmed to 55°C for 20 min to evaporate the residual ether. Portions were acetylated and analyzed for cGMP concentration by radioimmunoassay according to the manufacturer's instructions (Biomedical Technologies). Results are expressed as the mean of triplicate determinations ± SEM.

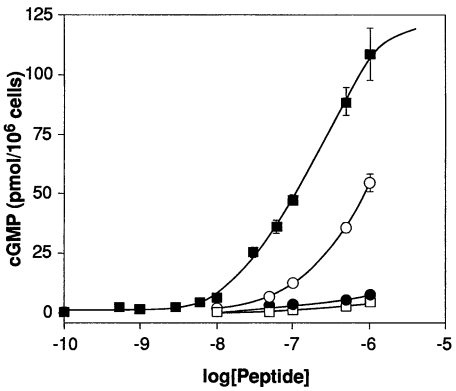

Fig. 2. Concentration-dependent stimulation of the ANPR-B guanylyl cyclase by natriuretic peptides. COS-7 cells were plated and transfected with the ANPR-B expression plasmid as in Fig. 1. The cells were washed and incubated as above and stimulated with or without varying concentrations of natriuretic peptides [hCNP (■), hANP (●), hBNP (□), and pBNP (○)]. Intracellular cGMP accumulation was determined as in Fig. 1. Each point represents the mean of triplicate samples assayed in duplicate (± SEM).

GC-A and GC-B) are approximately 1030–amino acid transmembrane guanylyl cyclases (*9–12*). The third receptor, ANPR-C, is a 496–amino acid transmembrane protein with a short 37–amino acid cytoplasmic tail (*13, 14*). This receptor, also called the clearance receptor (*15*), does not signal through activation of guanylyl cyclase, but may function through intermediate G proteins to inhibit adenylyl cyclase or activate the phosphoinositol pathway (*16*). ANPR-C imposes the fewest structural constraints of all the receptors on ligands it will recognize in a binding assay (*17*). ANP is the most potent hormone for stimulation of the ANPR-A guanylyl cyclase; BNP is as efficacious, but only at approximately tenfold higher concentrations (*12*). The ANPR-B guanylyl cyclase, on the other hand, produces only low amounts of cGMP after activation by relatively high concentrations of ANP or BNP (*11, 12*). These experiments suggest either that ANPR-B signals through a second messenger system other than cGMP or that the natural ligand recognized by ANPR-B has not been described. With these results in mind, we studied the ability of the recently described natriuretic peptide, human CNP (hCNP) (*18*), to bind to and activate the guanylyl cyclase of the cloned human A and B receptors expressed in mammalian cells.

Expression vectors in which human ANPR-A and ANPR-B are under the control of the cytomegalovirus immediate early promoter (*10, 11*) were transfected into COS-7 cells. Intracellular cGMP content was determined after the intact cells were incubated in the presence of hCNP or the natriuretic peptides known to stimulate the ANPR-A and ANPR-B guanylyl cyclases most effectively (*11*); that is, human ANP (hANP) and porcine BNP (pBNP) (*19*), respectively (Fig. 1). In cells transfected with a control expression vector alone, less than 2 pmol of cGMP per 10^6 cells was detectable with or without hormone stimulation. As previously shown (*11*), hANP and pBNP markedly increased cGMP accumulation in ANPR-A–expressing cells (58.6 ± 1.4 and 44.6 ± 3.1 pmol per 10^6 cells, respectively) above nonstimulated concentrations (1.5 ± 0.1 pmol per 10^6 cells). For ANPR-B–expressing cells, cGMP concentrations increased 5-fold with hANP stimulation and 30-fold with pBNP stimulation. The hCNP displayed a much greater selectivity for stimulating the guanylyl cyclase activity of these receptors. In cells expressing ANPR-A, hCNP stimulation did not increase intracellular cGMP. Conversely, in ANPR-B–expressing cells, hCNP elicited the highest guanylyl cyclase activity (56.1 ± 3.6 pmol of cGMP per 10^6 cells), which is comparable to that seen when ANPR-A–expressing cells were stimulated with hANP.

Comparative dose-response experiments were performed on cells expressing ANPR-B to study the kinetics of guanylyl cyclase activation (Fig. 2). Over the concentrations tested, hANP and hBNP increased cGMP only slightly. The pBNP caused a dose-dependent increase in cGMP production, but very high, nonphysiological concentrations were needed to produce this effect. In contrast, hCNP elicited a classic dose-dependent increase in cGMP. The half-maximal effective concentration (EC_{50}) was estimated at 100 nM; however, there was a significant increase in cGMP over background at concentrations as low as 0.5 nM (1.69 ± 0.05 versus 1.33 ± 0.03 pmol per 10^6 cells; $P < 0.05$). Therefore, CNP selectively activated the guanylyl cyclase of ANPR-B at physiologically relevant concentrations and with a kinetic profile typical of a natural ligand.

To determine whether the activation of the guanylyl cyclase correlates with the bind-

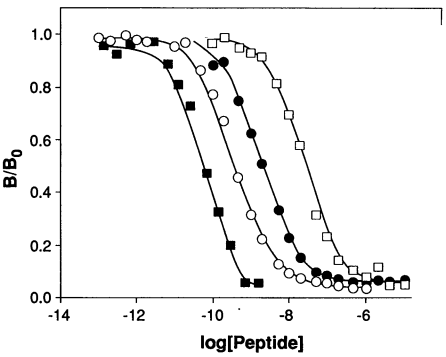

Fig. 3. Inhibition of the specific binding of [^{125}I]CNP by natriuretic peptides to cells expressing the binding domain of ANPR-B. Human embryonic kidney cells stably expressing the extracellular and transmembrane domain of ANPR-B (*21*) were harvested with phosphate-buffered saline (PBS) + 5 mM EDTA and washed with PBS containing 0.1% bovine serum albumin and 0.02% sodium azide (PBSA buffer). Duplicate samples of 10^4 cells in 1 ml of PBSA were incubated at room temperature for 2 hours while shaking with 15 pM [^{125}I]CNP (*20*) alone or in the presence of increasing concentrations of unlabeled hCNP (■), hANP (●), hBNP (□), and pBNP (○). Nonspecific binding was determined by addition of 10^{-5} M displacing peptide. The assay was terminated by rapid filtration through Millipore GF/C filters followed by washing with PBSA, and the amount of bound ^{125}I was determined by counting the filters in a gamma counter. The data were analyzed by the LIGAND program of Munson and Rodbard (*28*). Results are expressed as the counts per minute specifically bound at each peptide concentration (B) divided by the counts per minute specifically bound in the absence of displacing peptide (B_0).

ing of CNP to ANPR-B, [^{125}I]CNP (*20*) was incubated with human embryonic kidney (293) cells stably expressing the extracellular and transmembrane domains of ANPR-B (*21*) in the presence of competing concentrations of hANP, hBNP, pBNP, or hCNP (Fig. 3). The rank order of potency for binding to those sites labeled by [^{125}I]CNP was the same as for stimulating the ANPR-B guanylyl cyclase; that is, hCNP > pBNP > hANP > hBNP. The inhibition constant (K_i) values for these ligands were 30 pM, 0.3 nM, 1.6 nM, and 14.7 nM, respectively. Therefore, in both binding and guanylyl cyclase activation studies, the most potent hormone interaction with ANPR-B was by hCNP.

No specific binding of [^{125}I]CNP was seen to cells expressing either the extracellular domain or the full-length ANPR-A protein (*22*). Also, hCNP did not significantly displace [^{125}I]ANP bound to these cells [median inhibitory concentration (IC_{50}) > 1 μM] (*22*). To determine the selectivity of hCNP binding to the ANPR-C protein, we measured the ability of hCNP to displace [^{125}I]ANP from 293 cells stably expressing human ANPR-C (*14, 22*). The rank order of potency for the hormones used was pBNP > hANP ≥ hCNP > hBNP with K_i values of 97 pM, 0.12 nM, 0.14 nM, and 3.7 nM, respectively. Thus, in binding studies, ANPR-C recognized all the natriuretic peptides including CNP; however, its affinity for CNP was fivefold lower than that of ANPR-B.

Our data elucidate the important receptor-ligand interactions within the natriuretic peptide and receptor families. The hormone specificity for activation of the guanylyl cyclases of ANPR-A and ANPR-B or for binding to ANPR-C in humans is represented in Fig. 4 (*23*). The ANPR-A guanylyl cyclase is activated most efficiently by ANP. BNP is also effective at stimulating this cyclase but is approximately tenfold less potent (*12*). Studies have suggested that although the release of these two cardiac hormones is subject to differential regulation (*24*), they have similar physiological activities (*2, 7, 25*). Therefore, their effects may be mediated through the same receptor; that is, ANPR-A. Alternatively, there may be an as yet unidentified member of the natriuretic peptide receptor guanylyl cyclase family that is specifically activated by BNP. ANPR-C can recognize a remarkable diversity of natriuretic hormones and analogs (*17, 22*), and all three of the known human natriuretic peptides bind the human receptor with affinities in the low nanomolar range.

The experiments described here illustrate that the newest member of the natriuretic peptide family, CNP, selectively binds and activates the human ANPR-B protein. No other human natriuretic peptide was able to substantially stimulate the guanylyl cyclase of this receptor, and the binding affinity of hCNP was 50- to 500-fold greater than the other human natriuretic peptides. Since CNP is significantly less potent at inducing natriuretic, diuretic, and hypotensive effects in vivo than either ANP or BNP (*2, 4*), it is possible that its primary biological activity is not as a classic natriuretic peptide with peripheral sites of action. Preliminary experiments on the distribution of CNP mRNA by Northern analysis (*5*) and ANPR-B mRNA by in situ hybridization (*26*) suggest that the localization of these two species is limited primarily to the nervous system or to cells derived from the neural crest. Studies of intracerebral injections of ANP or BNP in the rat suggest that natriuretic peptides in the brain may be involved in the regulation of the activity of the vasopressin and angiotensin hypothalamic systems to maintain proper body fluid homeostasis (*27*). CNP is presumed to be the natriuretic peptide with the highest concentration in the brain (*5, 8, 18*); therefore, although extensive experiments with CNP in the brain are necessary, it is possible that CNP, acting through ANPR-B, is responsible for most of the central effects presently attributed to natriuretic peptides. Further studies on the physiology and binding characteristics of CNP and ANPR-B in the brain should help clarify their roles in the central nervous system.

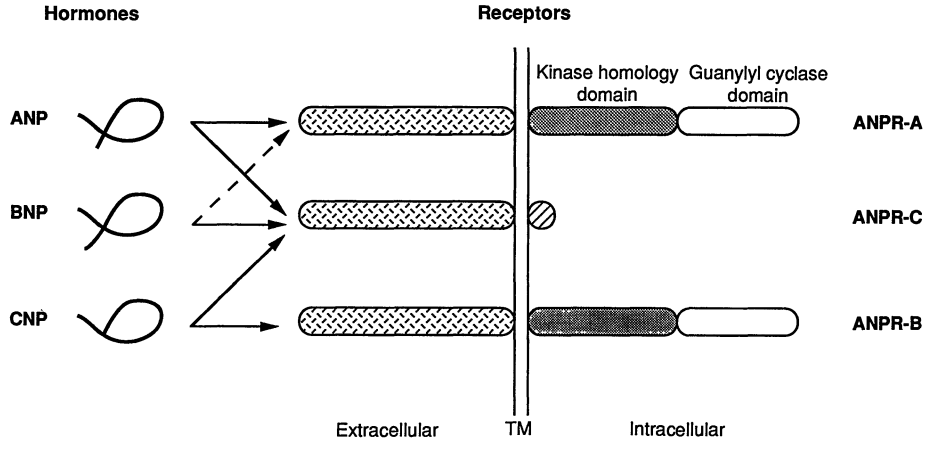

Fig. 4. Hormone specificity for the human natriuretic peptide receptors. A schematic representation of the ability of the human natriuretic peptides to specifically activate the guanylyl cyclase of human ANPR-A or ANPR-B or bind to human ANPR-C. The solid lines connect the receptors with their preferred ligand. The ambiguity of BNP's role in activation of ANPR-A is represented by a dashed line, as described in the text. TM, transmembrane region.

REFERENCES AND NOTES

1. T. Inagami, *J. Biol. Chem.* **264**, 3043 (1989); J. D. Baxter, J. A. Lewicki, D. G. Gardner, *Biotechnology* **6**, 529 (1988).
2. T. Sudoh, K. Kangawa, N. Minamino, H. Matsuo, *Nature* **332**, 78 (1988).
3. Y. Kambayashi *et al.*, *FEBS Lett.* **259**, 341 (1990).
4. T. Sudoh, N. Minamino, K. Kangawa, H. Matsuo, *Biochem. Biophys. Res. Commun.* **168**, 863 (1990).
5. M. Kojima, N. Minamino, K. Kangawa, H. Matsuo, *FEBS Lett.* **276**, 209 (1990).
6. ———, *Biochem. Biophys. Res. Commun.* **159**, 1420 (1989); T. Sudoh *et al.*, *ibid.*, p. 1427.
7. D.-L. Song, K. P. Kohse, F. Murad, *FEBS Lett.* **232**, 125 (1988).
8. M. Furuya *et al.*, *Biochem. Biophys. Res. Commun.* **170**, 201 (1990).
9. M. Chinkers *et al.*, *Nature* **338**, 78 (1989).
10. D. G. Lowe *et al.*, *EMBO J.* **8**, 1377 (1989).
11. M.-S. Chang *et al.*, *Nature* **341**, 68 (1989).
12. S. Schulz *et al.*, *Cell* **58**, 1155 (1989).
13. F. Fuller *et al.*, *J. Biol. Chem.* **263**, 9395 (1988).
14. D. G. Lowe, T. R. Camerato, D. V. Goeddel, *Nucleic Acids Res.* **18**, 3412 (1990).
15. T. Maack *et al.*, *Science* **238**, 675 (1987).
16. M. B. Anand-Srivastava, A. K. Srivastava, M. Cantin, *J. Biol. Chem.* **262**, 4931 (1987); M. B. Anand-Srivastava, M. R. Sairam, M. Cantin, *ibid.* **265**, 8566 (1990); M. Hirata, C. H. Chang, F. Murad, *Biochim. Biophys. Acta* **1010**, 346 (1989).
17. P. R. Bovy, *Med. Res. Rev.* **10**, 115 (1990).
18. We used CNP-22 for all the studies reported here because this was the form of the peptide first isolated from porcine brain (*4*). An NH_2-terminally extended form of CNP (CNP-53) has been characterized [N. Minamino, K. Kangawa, H. Matsuo, *Biochem. Biophys. Res. Commun.* **170**, 973 (1990)]. Preliminary experiments demonstrated that these two analogs had comparable biological activity. Gene and mRNA analysis of these peptides across species has shown that porcine and rat CNP-53 are identical and that there are two amino acid substitutions in the NH_2-terminal portion of human CNP-53. In addition, initial radioimmunoassay results suggest that CNP-53 may be the predominant form of CNP present in porcine brain with a concentration three to five times that of CNP-22 (N. Minamino, K. Kangawa, H. Matsuo, unpublished observations).
19. The 26–amino acid version of pBNP was used for all experiments in this study.
20. Both CNP and its NH_2-terminally extended analog, Tyr^0-CNP, were synthesized by solid-phase techniques as previously described (*4, 8*). The ability of Tyr^0-CNP to stimulate guanylyl cyclase activity in both ANPR-A– and ANPR-B–expressing cells was equivalent to that of hCNP, suggesting they interact with the same cell surface receptor and that the additional tyrosine does not affect the biological activity of CNP (K. J. Koller *et al.*, unpublished observations). Tyr^0-CNP was labeled with $Na^{125}I$ and lactoperoxidase, and the monoiodinated Tyr^0-CNP product, [^{125}I]CNP, was purified by reversed-phase high-performance liquid chromatography [A.

Miyata, K. Kangawa, T. Toshimori, T. Hatoh, H. Matsuo, *Biochem. Biophys. Res. Commun.* **129**, 248 (1985)]. Mass spectrometry of products from a nonradioactive labeling reaction was used to confirm the structure of iodinated Tyr^0-CNP.
21. The cells stably expressing the extracellular binding and transmembrane domains of ANPR-B that were used for binding studies express up to 1000 times more sites per cell than cells expressing the full-length receptor, either transiently in COS-7 cells or stably in 293 cells (*22*). This high degree of expression of the binding domain of the protein facilitated the subsequent binding assays by dramatically increasing the signal-to-noise ratio of the assay. [^{125}I]CNP binding isotherms on cells expressing the full-length ANPR-B or the truncated protein suggested that the affinity of CNP for both forms of the receptor was of a similar magnitude (*22*). Unfavorable signal-to-noise ratios for binding to intact ANPR-B precluded quantitative analysis.
22. D. G. Lowe *et al.*, unpublished observations.
23. It is possible that in other species, such as rat or pig, the natriuretic peptides may not display the same receptor preferences as in human. Similar studies on stimulation of the rat ANPR-A and ANPR-B guanylyl cyclases with CNP should help clarify this point. In addition, pBNP, which has some ability to stimulate human ANPR-B, may be a potent activator of the porcine ANPR-B.
24. M. Mukoyama *et al., N. Engl. J. Med.* **323**, 757 (1990).
25. A. McGregor, M. Richards, E. Espiner, T. Yandle, H. Ikram, *J. Clin. Endocrinol. Metab.* **70**, 1103 (1990).
26. J. N. Wilcox, A. Augustine, D. V. Goeddel, D. G. Lowe, in preparation.
27. J.-G. Chabot, G. Morel, R. Quirion, in *Current Aspects of the Neurosciences*, N. N. Osborne, Ed. (Macmillan, London, 1990), vol. 1, chap. 2.
28. P. Munson and D. Rodbard, *Anal. Biochem.* **107**, 220 (1980).
29. We thank C. Quan, M. Struble, and J. Burnier for peptide synthesis and purification; S. Wong for amino acid analysis; J. Bourell for mass spectrometric analysis; A. Renner for technical assistance; C. Morita, K. Andow, and L. Tamayo for help with computer graphics; and R. Vandlen for helpful discussions.

11 October 1990; accepted 23 January 1991

Spiral Calcium Wave Propagation and Annihilation in *Xenopus laevis* Oocytes

JAMES LECHLEITER, STEVEN GIRARD, ERNEST PERALTA, DAVID CLAPHAM*

Intracellular calcium (Ca^{2+}) is a ubiquitous second messenger. Information is encoded in the magnitude, frequency, and spatial organization of changes in the concentration of cytosolic free Ca^{2+}. Regenerative spiral waves of release of free Ca^{2+} were observed by confocal microscopy in *Xenopus laevis* oocytes expressing muscarinic acetylcholine receptor subtypes. This pattern of Ca^{2+} activity is characteristic of an intracellular milieu that behaves as a regenerative excitable medium. The minimal critical radius for propagation of focal Ca^{2+} waves (10.4 micrometers) and the effective diffusion constant for the excitation signal (2.3×10^{-6} square centimeters per second) were estimated from measurements of velocity and curvature of circular wavefronts expanding from foci. By modeling Ca^{2+} release with cellular automata, the absolute refractory period for Ca^{2+} stores (4.7 seconds) was determined. Other phenomena expected of an excitable medium, such as wave propagation of undiminished amplitude and annihilation of colliding wavefronts, were observed.

MANY G PROTEIN–LINKED RECEPTORS stimulate a common cell signaling pathway leading to activation of phospholipase C (PLC), release of diacylglycerol and inositol 1,4,5-trisphosphate (IP_3), and the subsequent IP_3-induced release of intracellular Ca^{2+} (*1*). The specificity of signal transduction by these receptors may be preserved by the spatiotemporal pattern of changes in the concentration of intracellular free Ca^{2+} ($[Ca^{2+}]_i$) (*2*). Consequently, we have examined such spatiotemporal patterns of release of free Ca^{2+} in the cytoplasm of *Xenopus* oocytes expressing muscarinic acetylcholine receptors (mAChRs), which are known to be coupled to turnover of phosphatidylinositol. The *Xenopus* oocyte is a valuable model for studying Ca^{2+} signaling. Changes in $[Ca^{2+}]_i$ have been followed by measuring the intrinsic Ca^{2+}-activated chloride ($I_{Ca,Cl}$) currents and by imaging with Ca^{2+}-sensitive dyes. Qualitatively different patterns of release of free Ca^{2+} have been observed in *Xenopus* oocytes, ranging from regenerative focal release to oscillations or propagating plane waves (*3, 4*). Several models have been proposed to explain the complex patterns of Ca^{2+} release. Oscillations in $[Ca^{2+}]_i$ may result from Ca^{2+}-induced Ca^{2+} release (CICR), while IP_3 remains constant, or from feedback mechanisms on PLC activity that cause IP_3 levels to vary (*5*). Since oscillatory $I_{Ca,Cl}$ currents have been observed in *Xenopus* oocytes with nonhydrolyzable analogs of IP_3 (*6*), the CICR hypothesis has recently gained factor.

Oocytes were used 48 hours after injection of mAChR transcripts (*4*) and were injected with the Ca^{2+} dye indicator fluo-3 (50 nl of 1 mM; ~50 μM final concentration) 30 to 120 minutes prior to each experiment. Confocal imaging of a single optical slice, close to the plasma membrane surface of each oocyte, was repeated at 1-s intervals. A two-electrode voltage clamp of $I_{Ca,Cl}$ was used in parallel with imaging to monitor Ca^{2+} release both within and distal to the imaging plane of the confocal microscope. As previously described, we found that the pattern of Ca^{2+} release induced by acetylcholine (ACh) was generally a propagating planar wave with velocities of 10 to 30 μm/s (*4*). This pattern of Ca^{2+} release was always accompanied by a rapid stimulation of $I_{Ca,Cl}$. In 14 of 30 oocytes, however, a more complex pattern of Ca^{2+} release was also observed—the occurrence of pulsating foci that produced circularly propagating Ca^{2+} waves. These regenerative patterns of Ca^{2+} release were observed at low ACh concentrations (10 nM) and at maximal ACh concentrations (1 to 50 μM), after the initial planar wave of Ca^{2+} had traveled through the imaging plane. At times, these regenerative waves of circular propagation would alter their pattern of propagation and change, from pulsating foci, into continuously cycling spiral waves of Ca^{2+} release (4 of 14 oocytes) (Fig. 1). The oocyte shown was stimulated with 1 μM ACh and exhibited the rapid $I_{Ca,Cl}$ current spike characteristic of mAChR responses (*4*). Approximately 2 min after ACh was applied to the oocyte, pulsatile focal Ca^{2+} release was observed and several of these foci developed into spiral waves. This complex pattern of Ca^{2+} release would not have been discerned in electrophysiological recordings alone, since the spatial information of Ca^{2+} release is not measured by the two-electrode voltage clamp method. Five images, captured over a 10-s period, followed the dominant spiral through one complete revolution (Fig. 1A). The spiral nature of the wave of Ca^{2+} release is more apparent when only the active wavefront is shown, as determined by sequential subtraction (*7*; Fig. 1, B and C). The initial wavelength, defined as the distance between the tangent of the spiral tip and the parallel tangent of the most adjacent wavefront, was ~210 μm.

The full regenerative character and the three-dimensional nature of spiral wave

J. Lechleiter, S. Girard, D. Clapham, Department of Pharmacology, Mayo Foundation, Rochester, MN 55905. E. Peralta, Department of Biochemistry and Molecular Biology, Harvard University, Cambridge, MA 02138.

*To whom correspondence should be addressed.